Adaptive post-earthquake reliability assessment of structures subjected to aftershocks

H. Ebrahimian, F. Jalayer & D. Asprone
Department of Structures for Engineering and Architecture, University of Naples Federico II, Naples, Italy

A.M. Lombardi & W. Marzocchi
Istituto Nazionale di Geofisica e Vulcanologia (INGV), Rome, Italy

A. Prota & G. Manfredi
Department of Structures for Engineering and Architecture, University of Naples Federico II, Naples, Italy

ABSTRACT: This study presents a methodology for operational time-dependent seismic aftershock risk forecasting as a support for rapid decision-making in a post main-shock environment. This issue is addressed herein by calculating the mean daily rate of exceeding a set of discrete limit states by convolving the associated time-dependent fragility curves with the daily aftershock hazard forecasts. Two alternative aftershock occurrence models, namely, the modified Omori's model (MO) and the epidemic type aftershock sequence (ETAS) are adopted. The Bayesian updating is used to provide sequence-based parameter estimates for the MO model as well as the ground motion prediction equation. In addition, a new methodology for adaptive time- and event-dependent fragility assessment is explored in this work. As a numerical example, daily forecasts of the aftershock risk are estimated for an equivalent single-degree-of-freedom structure subjected to the L'Aquila 2009 aftershock sequence (central Italy).

1 INTRODUCTION

Adaptive time-dependent seismic aftershock risk assessment can be a crucial analytic support for establishing transparent protocols for civil and structural protections in the presence of an ongoing aftershock sequence. In such a context, adaptive forecasting of daily rates of exceeding the ground motion intensity of interest (hazard) are going to be convolved with adaptive forecasting of daily fragility curves in order to predict the seismic aftershock risk.

This work presents how the information (the catalog and the waveforms) provided by the ongoing aftershock sequence can be used adaptively in order to make time-dependent aftershock risk assessment. The time-dependent probabilistic aftershock hazard assessment (PASHA) relies mainly on an aftershock occurrence model and a suitable ground motion prediction equation (GMPE). This work employs two established aftershock models, namely the Epidemic Type Aftershock Sequence (ETAS, Ogata 1998) and the modified Omori (MO, Utsu 1961). The modified Omori model attributes simple power-law decay to the temporal evolution of an aftershock sequence, taking into account only the triggering effect of the main-shock. This is while the ETAS model takes into account also the triggering effect of the aftershocks and capture the spatio-temporal evolution of the sequence. Although simplistic, the MO has been used quite often for PASHA (Gerstenberger et al. (2005), Yeo & Cornell 2009, Jalayer et al. 2011,

Goda & Taylor 2012). The ETAS model has been used for operational aftershock forecasting (Marzocchi & Lombardi 2009, Lombardi & Marzocchi 2010).

In this work, the modified Omori parameters are updated adaptively based on the catalog (time and magnitude) of the ongoing aftershock sequence, in a Bayesian framework. The Bayesian framework is used also to estimate the parameters of a strong GMPE based on the catalog and the wave-forms of the aftershock sequence.

As far as it regard the structural vulnerability assessment, the present study adapts the methodology presented by Jalayer et al. (2011) to an operational forecasting framework. A non-linear time-dependent performance variable, defined as the ratio of maximum demand increment to residual capacity, is adopted herein to represent the evolution in structural performance. Daily fragility curves are used to represent the time-dependent vulnerability of the structure, which are calculated as a sum of a sequence of (weighted) *event-based* fragility curves. The event-based fragilities are determined by a proposed approach, namely the *sequential cloud analysis* (Ebrahimian et al. 2013). Finally, the mean daily rate of exceeding a given limit state is calculated by integrating the daily rate of exceeding a given spectral acceleration (PASHA) and the daily fragility curve for the limit state in question. As a result, the forecasts associated with the mean daily rate of exceeding two limit states are obtained for the

L'Aquila aftershock sequence (central Italy). As the structural model, an equivalent SDOF model with cyclic strength and stiffness deterioration is used.

1.1 *The forecasting interval and the ongoing aftershock sequence*

In this work, the time interval $[T_{start}, T_{end}]$ within the particular jth day, $j=1,…, N_{day}$ (where N_{day} denotes the number of days considered for forecasting) is referred to as the "*forecasting interval*". In this work the forecasting interval last 24 hour and T_{start} is equal to 6AM UTC of the jth day. The aftershock events in the catalog taken place in the time elapsed after the main-shock until T_{start} are denoted as **seq,** used in the updating procedures described hereafter. Hereafter, the time-dependent background information $\mathbf{I}_j$, corresponding to the jth day, represents the **seq** of aftershock events with magnitudes greater than or equal to the lower cut-off magnitude M_l ($M \geq M_l$).

2 ALTERNATIVE MODELS FOR TIME-DEPENDENT SEISMICITY RATE

2.1 *The MO model*

Modified Omori's law is an empirical relation for the temporal decline of aftershock rates. With some modifications, Reasenberg & Jones (1989) proposed a simple comprehensive model to describe the aftershock occurrence based on MO model as a non-stationary Poisson process whose rate of exceedance of magnitude m, $\lambda_{MO}(t,m)$, decreases by roughly the reciprocal of time, t, elapsed after the main shock of magnitude M_m:

$$\lambda_{MO}\left(t,m\,|\,M_m\right) = \frac{10^{a+b(M_m-m)}}{\left(t+c\right)^p} \qquad (1)$$

where a, b, c and p = parameters of the MO model (see Lolli & Gasperini 2003 for more details). Accordingly, the number of aftershocks N_M from MO relation identified by vector $\mathbf{\theta}=[a,c,p]$, parameter b, following a main event, and considering $\mathbf{I}_j$, can be calculated by integrating Equation 1 as follows (ebrahimian et al., unpubl.):

$$N_M^{MO}\left(M\,|\,M_m,\mathbf{\theta},b,\mathbf{I}_j\right) = (10^{a+b(M_m-M_l)}-10^a)\cdot\mathrm{I}_0\left(T_{start},T_{end},c,p\right) \qquad (2)$$

where the term I_0 can be computed analytically:

$$\mathrm{I}_0\left(T_{start},T_{end},c,p\right) = \begin{cases} \left[\left(T_{end}+c\right)^{1-p}-\left(T_{start}+c\right)^{1-p}\right]/(1-p) & p \neq 1 \\ \ln\left[\left(T_{end}+c\right)/\left(T_{start}+c\right)\right] & p=1 \end{cases} \qquad (3)$$

2.2 *The ETAS model*

The ETAS Model is one of the most diffused class of models for short-term spatio-temporal forecasts

(Ogata, 1998, Marzocchi & Lombardi, 2009, Lombardi & Marzocchi 2010) which uses the observed regularity of earthquake occurrence data rather than using physical (tectonic, geological or geodetic) information, explicitly. The ETAS model is an epidemic stochastic point process in which every earthquake is a potential triggering event for subsequent earthquakes; thus, the seismicity is the superposition of those induced by previous events on the background.

The number of aftershock events N_M from ETAS model identified by vector of parameters $\mathbf{\theta}'$, following a main event, and considering $\mathbf{I}_j$, can be calculated as:

$$N_M^{ETAS}\left(M\,|\,M_m,\mathbf{\theta}',\mathbf{I}_j\right) = $$
$$\left(1-e^{-\beta(M_m-M_l)}\right)\int_{\Re}\mathrm{d}x\mathrm{d}y\int_{T_{start}}^{T_{end}}\lambda_{ETAS}\left(t,x,y,M_l\,|\mathbf{seq}\right)\mathrm{d}t \qquad (4)$$

where $\beta = b\ln(10)$; and $\lambda_{ETAS}(t,x,y,M_l|\mathbf{seq})$ = the conditional seismicity rate in space R(x,y) and time t, for $M \geq M_l$ given previous earthquakes (see Marzocchi & Lombardi 2009 for definition of the model parameters and its seismicity rate).

3 ADAPTIVE AFTERSHOCK FORECASTING USING BAYESIAN UPDATING

3.1 *General*

The posterior joint probability distribution (given the **seq**) for uncertain parameters generally denoted as the vector $\mathbf{\Phi}$, can be calculated by implementing the Bayes formula:

$$p\left(\mathbf{\Phi}\,|\mathbf{seq}\right) = p\left(\mathbf{seq}|\mathbf{\Phi}\right)p\left(\mathbf{\Phi}\right)\Big/\sum_{\mathbf{\Phi}}p\left(\mathbf{seq}|\mathbf{\Phi}\right)p\left(\mathbf{\Phi}\right) \qquad (5)$$

where $p(\mathbf{\Phi}|\mathbf{seq})$ = posterior joint probability distributions; $p(\mathbf{\Phi})$ = prior joint probability distributions; and $p(\mathbf{seq}|\mathbf{\Phi})$ = the likelihood function given the general vector of parameters $\mathbf{\Phi}$. By applying the Bayesian updating adaptively to data provided by **seq**, the parameters of the MO model as well as the existing GMPE are daily estimated, as described in the subsequent sections.

3.2 *Adaptive Bayesian updating of MO parameters*

The parameters b and $\theta=[a,p,c]$ of the MO are estimated adaptively, following the procedure represented in Jalayer et al. 2011, using the Bayesian updating and conditioned on the time-dependent information represented by $\mathbf{I}_j$. Moreover, the lower cut-off magnitude M_l is verified adaptively by calculating the catalog completeness magnitude (Ebrahimian et al. unpubl.).

As a result, the number of aftershock events for jth day within the forecasting interval $[T_{start}, T_{end}]$ based on the MO model with updated parameters b and $\mathbf{\theta}$, can be calculated based on Equation 2.

3.3 Adaptive Bayesian updating of an existing strong-motion attenuation model

The parameters of the GMPE developed for strong-motions by Sabetta & Pugliese (1996) (herein as SP96) are updated adaptively based on the information provided by the **seq** in order to become applicable for the small-magnitude near-source ranges within the aftershock zone. However, the presented method can be applied to any other GMPE; the SP96 has been chosen due to its relatively simple formulation as well as its wide use for Italian territory.

The vector of coefficients of SP96 to be updated daily can be summarized as $\boldsymbol{\pi} = \{c_1, c_2, c_3, c_4, c_5, \sigma\}$, where c_1 = constant of regression; c_2 = coefficient of magnitude; c_3 = coefficient of epicentral distance; c_4, c_5 = coefficients of the site classification; and σ = standard deviation of the regression model. It is to note that these coefficients are related to logarithm (base 10) of pseudo spectral velocity (for more details see Sabetta & Pugliese 1996). With reference to Equation 5, $p(\boldsymbol{\pi}|\mathbf{seq})$ and $p(\boldsymbol{\pi})$ are the posterior and prior joint probability distributions, respectively, and $p(\mathbf{seq}|\boldsymbol{\pi})$ is the likelihood function for the aftershock sequence. Denoting by r_i: $i=1,\dots,N$ to be the epicentral distance (with respect to the desired site) for the ith event within the **seq** of N aftershocks, and assuming independence between consecutive events, the likelihood function $p(\mathbf{seq}|\boldsymbol{\pi})$ can be expressed as:

$$p(\mathbf{seq}|\boldsymbol{\pi}) = \prod_{i=1}^{N} p\left(Sa_i(T)\big|m_i, r_i, \boldsymbol{\pi}, \mathbf{I}_j\right) p\left(m_i, r_i | \mathbf{I}_j\right) \quad (6)$$

where $p(Sa_i(T)|m_i, r_i, \boldsymbol{\pi}, \mathbf{I}_j)$ = lognormal PDF of spectral acceleration of the ith aftershock wave-forms at the period of interest; $Sa_i(T)$: $i=1,\dots,N$ = spectral acceleration calculated based on the GMPE with the parameters $\boldsymbol{\pi}$, and information $\mathbf{I}_j$; and $p(m_i, r_i|\mathbf{I}_j)$ = the joint probability distribution of magnitude and distance, where $p(m_i, r_i|\mathbf{I}_j) = p(m_i|\mathbf{I}_j) p(r_i)$ assuming independence between magnitude and distance for areal seismogenetic zones; $p(m_i|\mathbf{I}_j) = p(m_i|b, \mathbf{I}_j)$ is the truncated Gutenberg probability density function $(M_l \le m \le M_m)$; $p(r_i)$ = the marginal probability distribution for distance and is assumed constant herein (i.e., spatially invariant seismicity with Cartesian areal increments), only for the updating purposes.

By substituting Equation 6 into the Bayesian formulation, i.e. Equation 5, one can calculate the MLE of the vector of parameters $\boldsymbol{\pi}_{\mathrm{mle}}$ based on the joint posterior $p(\boldsymbol{\pi}|\mathbf{seq})$. $\boldsymbol{\pi}_{\mathrm{mle}}$ can be interpreted as the adaptively updated attenuation parameters for the ongoing aftershock sequence.

4 ADAPTIVE PROBABILISTIC SEISMIC AFTERSHOCK HAZARD ANALYSIS

The mean daily rate of exceeding a given spectral acceleration at a specified period $Sa(T)$ can be calculated by integrating the daily forecasts for occurrence model and the daily updated GMPE:

$$\lambda\left(Sa(T) > x | \mathbf{I}_j\right) = N_M(M|\mathbf{I}_j) \cdot$$
$$\iint_{m\ \mathfrak{R}} P\left[Sa(T) > x \big| m, r, \mathbf{I}_j\right] p(m, r | \mathbf{I}_j)\,\mathrm{dx dy}\,\mathrm{d}m \quad (7)$$

where $\lambda(x|\mathbf{I}_j)$ = the time-dependent daily rate that $Sa(T)$ exceeds a given value x for the jth day given $\mathbf{I}_j$; N_M = the number of forecasted aftershocks (Equation 2 for MO model and Equation 4 for ETAS model); $P[Sa(T)>x|m,r,\mathbf{I}_j]$ = the daily updated probability model for ground motion prediction in terms of $Sa(T)$ calculated as a function of the daily best-estimates $\boldsymbol{\pi}_{\mathrm{mle}}$; $p(m,r|\mathbf{I}_j)$ = the joint probability of the magnitude and distance (as described in Section 3.3); however, it is to note that the updated b parameter for calculating $p(m|\mathbf{I}_j)$ is estimated daily; r = epicentral distance over the entire aftershock zone $\mathfrak{R}(x,y)$ with respect to the location of the desired site; and $p(r_i)$ = the probability density function for distance obtained by (1) the spatio-temporal evolution of the seismicity in ETAS model, (2) spatially uniform for MO model.

5 TIME-DEPENDENT VULNERABILITY ASSESSMENT

5.1 Structural performance variable

Assume that N_{as} events take place in the forecasting interval associated with the particular jth day. Each event n: $n=1,\dots,N_{as}$ tends to increase the peak and residual drift demands. Hence, the structural response to the nth event might be significantly affected by the residual drift demands due to $(n-1)$ previous events. Herein, a novel scalar time-dependent performance variable, Y_{LS}, is introduced as the ratio of maximum demand increment due to the sequence of n events and the residual drift capacity (see Ebrahimian et al. 2013):

$$Y_{LS}^{(n)} = \frac{D_{\max}^{(n)} - D_{\mathrm{r}}^{(n-1)}}{C_{LS} - D_{\mathrm{r}}^{(n-1)}} \quad (8)$$

where $D_{\max}$ = maximum drift demand due to the sequence of n events; D_{r} = residual drift demand corresponding to the sequence of $(n-1)$ events; C_{LS} is the capacity of the system for the desired limit state, LS. Accordingly, the first time within the sequence, where Y_{LS} becomes equal or greater than unity denotes the first-excursion of the desired LS.

5.2 Time-dependent vulnerability assessment

The probability of exceeding a specified *LS* conditioned on a *Sa(T)* level equal to *x* (a.k.a. the structural fragility) given the information $\mathbf{I}_j$ for the forecasting time interval corresponding to the *j*th day, can be expressed as follows (see ebrahimian et al. 2013 for detailed derivation of the fragility expressions utilized herein):

$$P\left(Y_{LS} \geq 1 \mid x, \mathbf{I}_j\right) = \sum_{n=1}^{N_{as}} P\left(Y_{LS} \geq 1 \mid n, x, \mathbf{I}_j\right) P\left(n \mid \mathbf{I}_j\right) \quad (9)$$

where $P(Y_{LS} \geq 1 \mid x, n, \mathbf{I}_j)$ = the structural fragility associated with the first-excursion approach for exceeding the *LS* threshold given that exactly *n* events take place in the forecasting interval; $P(n \mid \mathbf{I}_j)$ = the probability that exactly *n* events take place.

The fragility $P(Y_{LS} \geq 1 \mid x, n, \mathbf{I}_j)$ in Equation 9 can be calculated by considering that the first-excursion of the limit state in events *k=1,2, ..., n* are a set of mutually exclusive and collectively exhaustive (MECE) events (Ebrahimian et al 2013):

$$P\left(Y_{LS} \geq 1 \mid x, n, \mathbf{I}_j\right) = \sum_{k=1}^{n} \left(P\left(C_k \mid \overline{C_1 C_2 \ldots C_{k-1}}, x, \mathbf{I}_j\right) \cdot \prod_{i=1}^{k-1} \left[1 - P\left(C_i \mid \overline{C_1 C_2 \ldots C_{i-1}}, x, \mathbf{I}_j\right) \right] \right) \quad (10)$$

where C_k indicates $Y_{LS} \geq 1$ after *k*th event, and correspondingly, the superscript line specifies its negation. The probability sequence $P(C_k \mid C_1 C_2 \ldots C_{k-1}, x, \mathbf{I}_j)$ within Equation 10 is estimated based on a novel methodology called "*the sequential cloud analysis*". This approach will be briefly described later.

In addition, $P(n \mid \mathbf{I}_j)$ in Equation 9 is estimated based on both MO and ETAS models. In order to estimate the probability distribution based on ETAS model, this paper utilizes the work performed by Marzocchi & Lombardi (2009). They simulated 500 different synthetic daily catalogs by using the "thinning method" proposed by Ogata (1998) in order to obtain various realizations of N_{as} for the forecasting time interval, and hence, provided an empirical density function for $P(n \mid \mathbf{I}_j)$. On the other hand, this probability distribution is also estimated by a non-homogenous Poisson probability distribution based on the updated MO model:

$$P\left(n \mid \mathbf{I}_j\right) = \left(N_M^{MO}\right)^n e^{-N_M^{MO}} / n! \quad (11)$$

where N_m is calculated from Equation 2 based on the daily updated parameters.

5.3 Time-dependent risk assessment

The daily rate of exceeding a prescribed limit state denoted by λ_{LS}, which is equal to the mean daily rate $Y_{LS} \geq 1$, for the *j*th day can be obtained by convolving time-dependent fragility and hazard, as follows:

$$\lambda_{LS} = \lambda\left(Y_{LS} \geq 1\right) = \int_x P\left(Y_{LS} \geq 1 \mid x, \mathbf{I}_j\right) \left| d\lambda\left(x \mid \mathbf{I}_j\right) \right| \quad (12)$$

where the time-dependent fragility $P(Y_{LS} \geq 1 \mid x, \mathbf{I}_j)$ is obtained from Equation 9, and the daily hazard $\lambda(x \mid \mathbf{I}_j)$ from Equation 7.

5.4 Sequential cloud analysis

The sequential cloud analysis procedure (Ebrahimian et al. 2013) leads to the calculation of the sequence of fragility terms $P(C_k \mid C_1 C_2 \ldots C_{k-1}, x, \mathbf{I}_j)$ within Equation 10. Starting from the structural model that is already subjected to the events within the **seq**, a number of $k=1:N_{seq}$ sequences of aftershocks in the forecasting time interval denoted as **seq**$_{gen}$ are generated. Each generated **seq**$_{gen}$ consists of *k* waveforms, which are sequentially ordered by random permutation (with replacement) of the wave-forms recorded in the (available sequence) **seq**. While the structure is subjected to N_{seq} suites of **seq**$_{gen}$, a set of N_{seq} structural performance variables $Y_{LS}^{(k)}$, can be calculated. However, those $Y_{LS}^{(k)}$ values for which the structure has already exceeded the *LS* threshold in any of the previous events are not taken into account. By making the common assumption that the (conditional) distribution of Y_{LS} for a given level of *Sa(T)=x* can generally be described by a lognormal distribution, cloud analysis can be conducted (see Jalayer & Cornell 2003) for the *k*th fragility term in Equation 12:

$$P\left(C_k \mid \overline{C_1 C_2 \ldots C_{k-1}}, x, \mathbf{I}_j\right) = P\left(Y_{LS}^{(k)} \geq 1 \mid x, \mathbf{I}_j\right)$$
$$= 1 - \Phi\left(-\ln \eta_{Y|Sa}^{(k)}(x) / \beta_{Y|Sa}^{(k)}\right) \quad (13)$$

where $\eta_{Y|Sa}$ and $\sigma_{\ln Y|Sa} = \beta_{Y|Sa}$ are the conditional median and standard deviation of the natural logarithm of $Y_{LS}^{(k)}$, which can be obtained based on linear regression analysis (Jalayer & Cornell 2003, Jalayer et al. 2011).

6 NUMERICAL EXAMPLE

6.1 The L'Aquila aftershock sequence

On April 6, 2009, at 1:32 AM UTC, an earthquake with M_m=5.9 (local magnitude) struck central Italy in the Abruzzo region underneath the town of L'Aquila. The large shock triggered a vigorous aftershock sequence. The hypothetic site considered in this study is located near the recording station AQK (ITACA, http://itaca.mi.ingv.it/ItacaNet/). The reference building located on this site is a five-story RC frame structure, whose equivalent SDOF system has a period of 0.58s (see Section 6.5 for more details about the structural model). To generate operative daily aftershock occurrence forecasts based on ETAS and MO models (which are directly implemented in the PASHA), a provisional catalog used by Marzocchi & Lombardi (2009) is utilized herein. In addition to the catalog, the waveform archive of aftershock sequence was obtained as one of the

products related to the project "High-resolution multi-disciplinary monitoring of active fault test-site areas in Italy" (http://dpc-s5.rm.ingv.it/en/S5.html).

It has been investigated right after the main event (i.e. after the main-shock up to 6:00AM UTC of 06/04/09) , the completeness magnitude the catalog of aftershocks is estimated to be around 3 (local magnitude). Meanwhile, in all the subsequent days, the completeness magnitude is estimated around 2.5.

6.2 *The MO and ETAS models calibrated for the L'Aquila sequence*

The parameters of the MO model are estimated daily by applying a Bayesian updating routine to the L'Aquila 2009 sequence, as described in Section 3.2 (Ebrahimian et al. unpubl.). As prior probability distribution, the parameters estimated for the Italian generic aftershock sequence (Lolli and Gasperini, 2003) are considered.

The updated model parameters are then used to estimate the expected number of events based on Equation 2. Accordingly, the parameters of the ETAS model are calibrated for the L'Aquila sequence by Marzocchi & Lombardi (2009), which can directly be used for estimating the associated number of events based on Equation 4. The daily earthquake forecasts in terms of the number of events based on both MO and ETAS models are illustrated in Figure 1 for magnitude 2.5 and greater from April 6, 2009, at 6:00 UTC, a few hours after the main event up to May 10, 2009.
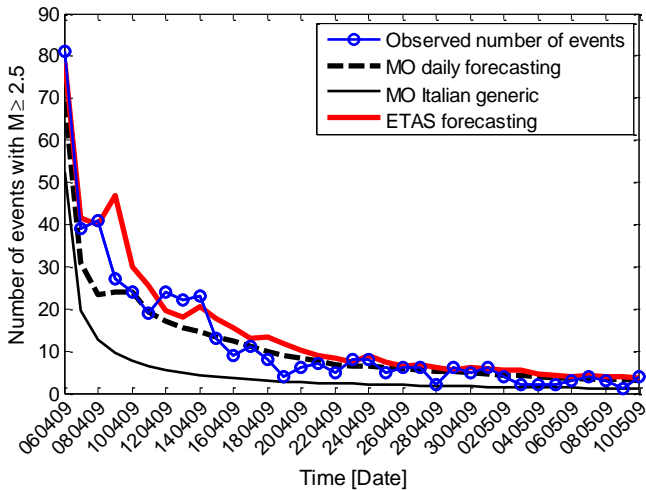
Figure 1. The daily observed and forecasted number of events, based on the MO and ETAS models.

For comparison, the real number of observed data in the catalog is shown, as well. It can be depicted that (1) both models perform quite well in capturing the trend in the number of aftershocks; (2) Although ETAS tends to provide an upper-bound estimate, it is more capable of predicting the instantaneous increase in the number of events; (3) adopting the Italian generic parameters for the MO model can cause

general underestimation. It should be noted that herein, the spatial issue related to the estimate of the number of predicted aftershocks are not studied and attention is focused on the implementations useful for hazard assessment.

6.3 *The GMPE calibrated for the L'Aquila sequence*

To estimate the updated parameters of SP96, the waveform archive of L'Aquila sequence is used in order to calculate the likelihood $p(\mathbf{seq}|\boldsymbol{\pi})$ based on Equation 6. Preliminary analyses on the distribution of Sa_i's with respect to their m_i's and r_i's revealed that the data did not reveal statistically significant trend versus distance; hence, the parameter c_3 of SP96 is not taken into account in the updating procedure. Furthermore, the hypothetic site is located on rock (type A); therefore, the parameters c_4 and c_5 are set to zero. This reduces the total number of parameters to be updated to three. It can be observed that the updated GMPE coefficients seem to converge to more-or-less stable values according to the evolution of the **seq** with time. Hence, the aftershock wave-forms registered in the first few days of the sequence seem to be adequate for updating the model parameters. Table 1 compares the original parameters of SP96 at the prescribed period T=0.58s with the sequence-specific maximum likelihood estimates (based on the posterior probability distribution) obtained based on the events taking place within the first 10 days after the main event. The large difference in the intercept parameter c_1 can be attributed to the fact that the distance-related coefficient is maintained fixed.

Table 1. Coefficients of SP96 model, T=0.58s

	c_1	c_2	σ
SP96	-0.762	0.530	0.295
MLE of posterior (15/04/09)	-2.670	0.880	0.235

6.4 *Forecasted aftershock hazard curves based on ETAS and MO*

Figure 2 illustrates the forecasted aftershock hazard curves expressed in terms of mean daily rate of exceeding various levels of $Sa(0.58s)$ for the date 06/04/09 corresponding to the first day, and $M_l \leq M \leq M_m$ for both ETAS and MO with adaptively updated parameters. The hazard values are calculated considering both the original SP96 parameters and those updated based on the wave-forms registered within the sequence. Moreover, the MO model is applied together with both a uniform spatial seismicity pattern and also a non-uniform time-invariable seismicity pattern. The non-uniform pattern is based on the ETAS-predicted spatial pattern

in the first day as a proxy for background seismicity spatial pattern.

Furthermore, the forecasted hazard curves are compared with the observed daily rate of exceedance of various spectral acceleration levels. This observed rate is calculated as the number of observed $Sa_i(T) > x$ of the aftershock wave-forms exceeding, which take place on the jth day within the forecasting time interval.
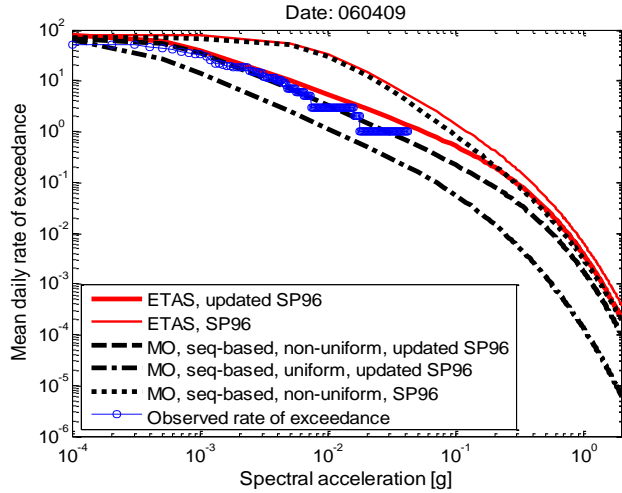
Figure 2. The forecasted hazard curves based on MO and ETAS, together with the observed exceedance rate in 06/04/2009, T=0.58s

The following observations can be depicted: (a) reasonable agreement between daily observed and forecasted hazard (ETAS, MO with time-invariant variable spatial seismicity); (b) MO with uniform seismicity systematically leads to under-estimations in the hazard prediction; (c) the significant improvements resulting from updating the parameters of the GMPE.

6.5 *The structural model and its limit states*

The case-study system is a modified version of the equivalent SDOF model which has been used by the authors in their previous works (see e.g. Jalayer et al. 2011, Ebrahimian et al. 2013). In this study, two discrete limit state are considered for the case-study structure, namely the Significant Damage (SD) and Near Collapse (NC), as outlined in Table 2. The LS's are distinguished herein in terms of increasing levels of the maximum displacement of the equivalent SDOF system. Preliminary analyses show that the structure is very close to the onset of the SD limit state due to the main-shock. Hence, this structure represents the structures that have experienced structural damage due the main-shock.

Table 2. LS's threshold for the equivalent SDOF

LS	Maximum Roof Drift (m)
Significant Damage (SD)	0.05
Near Collapse (NC)	0.07

OpenSees (http://opensees.berkeley.edu) is used for sequential nonlinear time history analyses by employing a hysteresis model with pinching that exhibits cyclic degradation in unloading and reloading stiffness as well as strength degradation (Pinching4 Material).

6.6 *Estimating N_{as} and $P(n/\mathbf{I}_j)$*

A best estimate for the maximum number of aftershock events within the forecasting time interval could be the (mean+1.7sigma) of the empirical distribution $P(n|\mathbf{I}_j)$ provided by ETAS (see Section 5.2). Subsequently $P(n|\mathbf{I}_j)$, n=1,…,N_{as}, can be obtained based on both ETAS and MO models (see Section 5.2 and Equation 11). For instance, N_{as} illustrating the maximum forecasted number of aftershock events with $M \geq 3.3$ is estimated to be equal to 15 for day 07/04/09 (Figure 4).
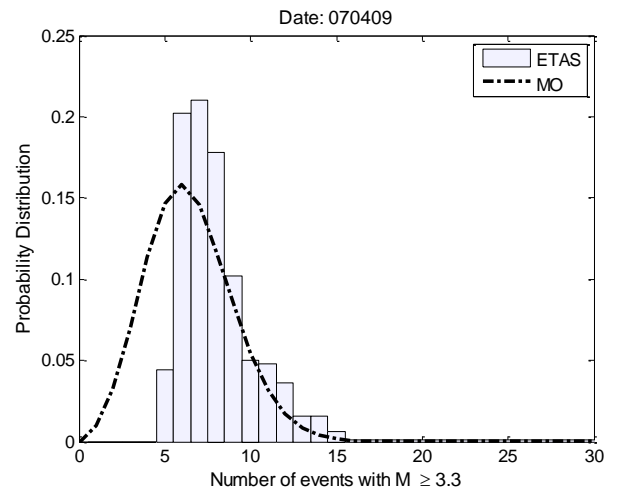
Figure 4. The forecasted distribution of the number of events per day (07/04/09) based on MO and ETAS models

It can be seen that the MO model assigns a non-zero probability to having very few aftershock events, while on the contrary, ETAS assigns zeros probability to those aftershock events. This is expected to affect the daily fragility curves which are going to be calculated through Equation 9 as a weighted sum of event-dependent fragilities.

6.7 *Daily fragility curves*

Figure 5 illustrates the increase in the structural vulnerability for DS (the first two days) and NC (the first four days) based on ETAS and MO models. It is important to note that the daily forecasts for each LS are provided up to the day in which the first-excursion takes place. For instance, the results for SD are only reported for the first two days elapsed after the main event (first excursion for SD takes place in the second day).

It can be observed through Figure 5 that the fragility curves obtained based on the two aftershock occurrence models are significantly different. The effect of the aftershock model on fragility estimation manifests itself through the probability distribution $P(n|\mathbf{I}_j)$, as explained in previous section. Consequently, the ETAS model systematically shifts the probability content towards larger number of aftershocks per day; hence, based on Equation 9, the event-dependent fragilities for larger n are going to have a larger weight. This leads to systematically larger fragility predictions based on ETAS compared to MO.

es from both the difference in the daily fragility and hazard forecasts. As a result, the MO model leads to systematically lower estimates; (2) the first-excursion of NC in the fourth day is accurately predicted by both models (as mean daily rate of exceedance equal to unity). However, the first-excursion of SD limit state in the second day is not signaled accurately. This can be attributed to the hazard forecasting. In particular, in the second day elapsed after the main event, another seismo-genetic structure became active and none of the two models managed to predict the hazard very well for this particular day.
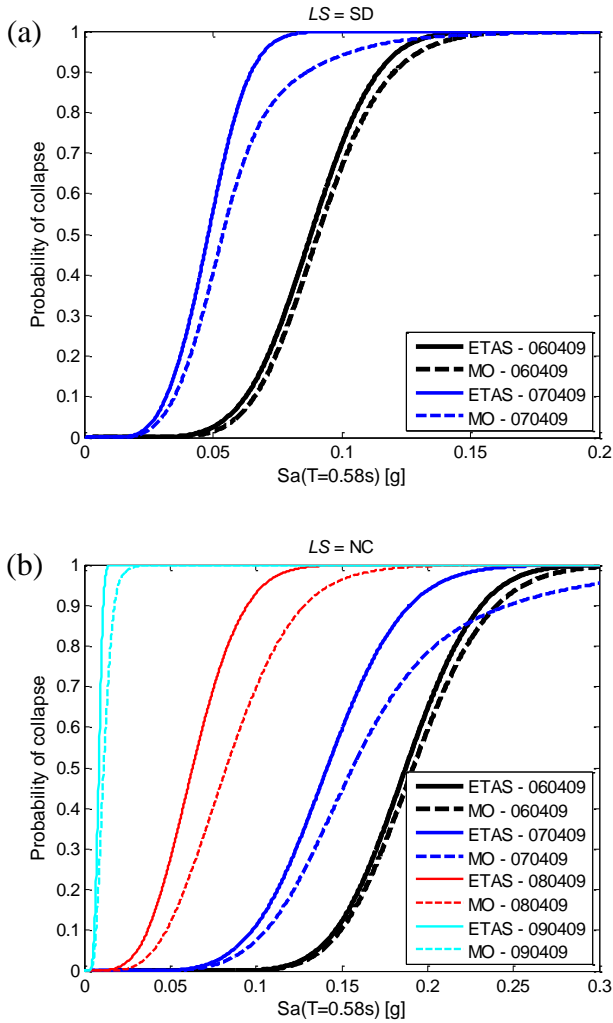
Figure 5. Forecasted daily-fragility curves (based on ETAS and MO models) for (a) SD, and (b) NC limit states

Figure 6. Daily risk forecasting for (a) SD, and (b) NC limit states based on ETAS and MO models

6.8 *Daily aftershock risk forecasting*

Daily aftershock risk, expressed in terms of the mean daily rate of exceeding limit states SD and NC, is calculated herein by the integration of the corresponding daily fragility and hazard curves, as shown in Equation 12. As a result, Figure 6 illustrates the daily risk forecasts for two both limit states SD and NC.

It can be observed that (1) the difference between the daily risk predictions based on both models aris-

7 CONCLUSION

This work outlines an adaptive framework for aftershock risk assessment based on information available from an on-going sequence. Daily forecasts of the aftershock risk are obtained by integration of daily predicted fragility and hazard curves. Two well-established models for the earthquake aftershock occurrence, namely, the modified Omori (MO) and the epidemic type aftershock sequence

(ETAS) are used herein. The seismic hazard in such a framework can be presented as the mean daily rates of exceeding various *Sa* values. The fragility curves are defined as the daily forecasted conditional first-excursion probabilities given *Sa* for the prescribed structural limit states. The information provided by the updated sequence (i.e., the catalog and the registered wave-forms) is used to: (a) update the parameters of the MO model using Bayesian updating; (b) update the parameters of a GMPE suitable for strong motion using Bayesian parameter estimation; (c) update the structural fragility for prescribed limit states.

In this methodology, the daily fragility curves are calculated as a weighted sum of event-dependent fragility curves, where the weights are equal to the probability that a given number of events take place. The event-based fragility curves are calculated next through a recursive formulation using a non-linear dynamic analysis procedure entitled sequential cloud analysis recently proposed by the authors (see Ebrahimian et al. 2013 for detailed description).

In general, the following observations can be made with regard to a case-study application associated with the L'Aquila 2009 seismic sequence:

• The mean daily rate of exceeding spectral acceleration (hazard) associated with ETAS and MO with a non-evolutionary spatially variable seismicity (based on updated GMPE) show reasonable agreement with the observed daily rates.

• The MO together with uniform spatial seismicity systematically under-estimates the hazard.

• The updating of the parameters of a strong-motion GMPE leads to significant improvement in the hazard estimations.

• The probability distributions for the number of aftershock events per day, which are used as weights in the calculation of daily fragilities, significantly affect the risk predictions.

• For the case-study structural system studied herein, risk forecasting based on both ETAS and MO models manages to properly capture the first-excursion of near collapse NC limit state in the fourth day elapsed after the main event. However, for the limit state of severe damage SD neither of the two methods can accurately predict the first-excursion in the second day. This may be attributed to the short-coming of both methods in predicting the seismic hazard in the second day, due to the activation of a second fault structure.

REFERENCES

Ebrahimian, H., Jalayer, F., Asprone, D., Lombardi, A.M., Marzocchi, W., Prota, A., Manfredi G. 2013. An outlook into time-dependent aftershock vulnerability assessment. In M. Papadrakakis, V. Papadopoulos, V. Plevris (eds.), *4th ECCOMAS Thematic Conference on Computational Methods in Structural Dynamics and Earthquake Engineering (COMPDYN2013)*, Kos Island, Greece, 12-14 June 2013.

Ebrahimian, H., Jalayer, F., Asprone, D., Lombardi, A.M., Marzocchi, W., Prota, A., Manfredi, G. 2013. Adaptive Daily Forecasting of Seismic Aftershock Hazard. *Bulletin of Seismological Society of America* (submitted).

Gerstenberger, M.C., Wiemer, S., Jones, L.M., Reasenberg P.A. 2005. Real-time forecasts of tomorrow's earthquakes in California. *Nature* 435: 328-331.

Goda, K. & Taylor, C.A. 2012. Effects of aftershocks on peak ductility demand due to strong ground motion records from shallow crustal earthquakes. *Earthquake Engineering and Structural Dynamics* 41(15): 2311-2330.

Jalayer, F. & Cornell, C.A. 2003. A Technical Framework for Probability-Based Demand and Capacity Factor Design (DCFD) Seismic Formats. *Pacific Earthquake Engineering Center* (*PEER*) 2003/08, November 2003.

Jalayer, F., Asprone, D., Prota, A., Manfredi, G. 2011. A decision support system for post-earthquake reliability assessment of structures subjected to aftershocks: an application to L'Aquila earthquake, 2009. *Bulletin of Earthquake Engineering* 9(4): 997-1014.

Lolli, B. & Gasperini, P. 2003. Aftershocks hazard in Italy part I: estimation of time-magnitude distribution model parameters and computation of probabilities of occurrence. *Journal of Seismology* 7(2): 235-257.

Lombardi, A.M. & Marzocchi, W. 2010. The ETAS model for daily forecasting of Italian seismicity in the CSEP experiment. *Annals of Geophysics* 53(3): 155-164.

Marzocchi, W. & Lombardi, A.M. 2009. Real-time forecasting following a damaging earthquake. *Geophysical Research Letters* 36 L21302, doi 10.1029/2009GL040233.

Ogata, Y. 1998. Space-time point-process models for earthquake occurrences. *Annals of the Institute of Statistical Mathematics* 50(2): 379-402.

Reasenberg, P.A. & Jones, L.M. 1989. Earthquake hazard after a mainshock in California. *Science* 243(4895): 1173-1176.

Sabetta, F. & Pugliese, A. 1996. Estimation of response spectra and simulation of nonstationary earthquake ground motions. *Bulletin of Seismological Society of America* 86(2): 337-352, 1996.

Utsu, T. 1961. A statistical study of the occurrence of aftershocks. *Geophysical Magazine* 30: 521-605.

Yeo, G.L. & Cornell, C.A. 2009. Post-quake decision analysis using dynamic programming. *Earthquake Engineering and Structural Dynamics* 38: 79-93.